

# Frequency Deviation Control Incorporating Fuzzy Plus Non-Integer PID Controller in EV Based Unified System

Sabita Tripathy\*, Manoj Kumar Debnath\*<sup>‡</sup>, Sanjeeb Kumar Kar\*

\* Department of Electrical Engineering, Siksha ‘O’ Anusandhan Deemed to be University, Bhubaneswar-751030, Odisha, India

(sabitatripathy@soa.ac.in, mkd.odisha@gmail.com, sanjeebkar@soa.ac.in)

<sup>‡</sup>Corresponding Author; Manoj Kumar Debnath, Siksha ‘O’ Anusandhan University, Bhubaneswar-751030, Odisha, India, Tel: +91 9040263931, mkd.odisha@gmail.com

Received: 08.02.2023 Accepted: 10.04.2023

**Abstract-** Different secondary controllers are necessary for Frequency deviation control to meet required power generation related to load demand. In this work a Fuzzy plus Non-Integer PID (FNPID) controller is projected for frequency deviation control in a unified system including EV (Electric Vehicle) aggregators. EVs are given priority because of its green environmental effect. Proper adjustment of gains of FNPID controller is also required to extract the best performance of the secondary controllers. Here a recent tuning process named as multi-verse optimizer (MVO) is applied for proper tuning of projected controller. The implemented dual area power system includes time varying delay-based EV aggregators and thermal generating units. The MVO technique is applied in the model to tune the controller constraints with abrupt application of load demand in one of the control areas. A time-based fitness function treated as ITAE (integral time absolute error) is applied to run the MVO algorithm. The dominance property of the projected FNPID controller over conventional Fuzzy-PID (FPID) and PID controller is observed in terms of different response specifications like maximum positive deviation (overshoot), settling time and minimum negative deviation (undershoot). The robust nature of the projected controller is also confirmed by multiple analysis like random load deviations and system constraints alteration.

**Keywords** Electric Vehicle, Controller Parameter Optimization, Frequency Deviation Control, Fuzzy Plus Non-Integer Controller, Multi-Verse Optimizer.

## Nomenclature/Abbreviation:

Symbol	Description	Abbreviation	Description
$T_{ev}$	EV time coefficient	GRC	Generation rate constraint
$K_{ev}$	EV gain factor	GDB	Governor dead band
$T_c$	Turbine time constant	TID	Tilt Integral derivative
$T_r$	Reheat time constant	MVO	Multi-verse optimizer
$F_p$	Reheat gain	EV	Electric Vehicle
$T_g$	Governor time constant	LFC	Load Frequency Control
$B$	Frequency bias coefficient	GA	Genetic algorithm
$M$	System inertia constant	ANFIS	Adaptive Neuro-Fuzzy Inference System
$D$	System damping constant	TCPS	Thyristor controlled phase shifter
$\alpha_1, \alpha_2$	Participation Factor	PSO	Particle swarm optimization
$T_{12}$	Tie-line power constant	SSSC	Static synchronous series compensator

<i>R</i>	Regulation time coefficient	ABC	Artificial bee colony
----------	-----------------------------	-----	-----------------------

**1. Introduction**

Power system mainly works on the balance between load demand and power generation. The unpredictable deviations in power demand leads to deviations of frequency in the unified system. The power generation should be maintained in accordance to power demand. The speed governor and secondary controllers in the generating plants mainly accounts for regulation of active power generation and hence frequency control in the unified power system [1-2]. The control loops in the power generating plant do the job of balance between active power generation and load demand.

Many research articles were published earlier to convey the importance of frequency regulation in interconnected power system. Initially conventional controllers [3-4] were used for LFC (load frequency control) in unified system for maintaining proper level of frequency. The implemented classical controllers were tuned by several optimization techniques. Afterwards fuzzy type controllers [5] were applied in interconnected plants for regulating frequency. The fuzzy controllers were self-tuned to accelerate the control action in the implemented model. Superconducting magnetic energy storage (SMES) device [6] was implemented in the interconnected hydro-thermal system for controlling system frequency. The tie-line decides the power exchange between the control areas during unpredictable load variations. The oscillations of interline power and area frequencies were analysed with the presence of TCPS (thyristor controlled phase shifter) in article [7]. Optimization techniques like Genetic Algorithm (GA) [8], Particle Swarm Optimization (PSO) [9] and chaotic optimization algorithm [10] were applied for successful tuning of gains of secondary controllers in unified system for frequency deviations control. Cam, et al. [11] applied fuzzy logic-based control methodology for regulation of frequency oscillations in unified power system during load fluctuations. The control of frequency deviations in interconnected control areas can be improved by hybridising fuzzy and neural network known as ANFIS (Adaptive Neuro-Fuzzy Inference System) [12]. Voltage control based on real time simulation in an unbalanced distribution system was performed by Ziadi, et. al. [13] with PV generating units. The performance of optimization techniques can be improved by the hybridisation of different algorithms. Debnath, et. al. [14] applied hybrid differential evolution–grey wolf optimization (DE-GWO) for better control of frequency deviations in interconnected power system. It is also evidenced by researchers that fractional controllers [15] are performing better related to integer control in the field of frequency regulation. In some cases filter component [16] is integrated with conventional controller for better performance in the control process. Participation of SSSC (Static synchronous series compensator) [17] improve the control techniques of frequency deviations in unified power system model. Solar-thermal units [18] and conventional thermal units were implemented for LFC analysis in multi-area power system. The existing tuning algorithm can also be modified for better tuning of constraints of controller. Sahu, et. al. [19] incorporated modified salp swarm optimization (SSO) for

proper tuning of fuzzy type-II controller gains in the examination of frequency deviation control. Hybrid PID-Fuzzy-PID controller is involved in article [20] for the investigation of frequency regulation in multi-area power system. Intelligent controllers like dual mode controller [21] also used by researchers for better management of frequency oscillations. Sliding mode controller tuned by ABC (artificial bee colony) technique is described in article [22] for LFC analysis in microgrids. Jaya algorithm tuned Solar-thermal units [23] are also involved by researchers in multi-generation system for frequency stability study. Fractional controller adjusted by dragonfly algorithm was employed in article [24] for effective control of frequency oscillations in unified power system. 3DOF-PID controller based on fractional calculus [25] was involved in multi-area system with renewable generating sources for LFC examination. Cascaded and fractional order controller tuned by WGA (wild goat algorithm) is deliberated in article [26] for frequency regulation study. An efficient tuning technique called Multi-verse optimizer was proposed by Mirjalili [27] to help the researchers for the optimization of different problems. Frequency abnormalities can also be controlled in multi-microgrid system [28] with the inclusion of storage devices. Non integer type modified controller named as TID (tilted integral derivative) controller is employed in article [29] for LFC in diverse-unit unified network. Kader, et al. [30] applied Plug-in-Hybrid Electric Vehicles (PHEVs) based on conventional controllers for LFC in unified system.

From the above survey it can be stated that many research articles have incorporated different control techniques for effective control of frequency deviations in multi-area unified power system. In this research paper fractional calculus is used along with fuzzy controller to develop Fuzzy plus Non-Integer PID Controller for frequency deviation regulation of unified power network. The following points highlighted the key contributions of the paper.

- Design of a unified system integrated with EV aggregators and thermal units for frequency deviation control.
- Application of fractional calculus to model Fuzzy plus Non-Integer PID (FNPID) Controller for LFC application.
- Tuning the projected controllers with the efficient multi-verse optimizer (MVO) technique.
- Establishing the dominance of implemented FNPID controller over FPID and PID controller in view of different response specifications like maximum positive deviation (overshoot), settling time and minimum negative deviation (undershoot).
- Validating the robustness of implemented FNPID controller by applying arbitrary demand variations and system constraint deviations.

**2. System Modelling**

Frequency deviation control analysis is become

essential with the application of EV aggregators. A large number of EVs are accounted as EV aggregators and employed along with other generating sources in multi-area system for frequency deviation control. The time delay of EV aggregators may results in the delay of system response because of which the stability of the system may be affected. In this research analysis a dual-area system is examined where EV aggregators are employed along with thermal generating power units in each area. GDB (Governor Dead Band) and GRC (Generation rate constraints) are also considered along with each thermal unit to make the system more practical. The examined model includes GRC of 3%/min for each thermal unit. For the GDB, 0.036 is considered as limiting value. The transfer function based model of the examined dual-area unified power system is illustrated in Fig.1. The nominal parameters of the model are stimulated from article [20] and are detailed in the appendix. The simplified transfer function of the EV aggregators [20] is presented by below equation.

$$G_{EV}(s) = \frac{K_{EV}}{1 + sT_{EV}}$$

Where the EV gain is denoted by  $K_{EV}$  and  $T_{EV}$  is the battery based time co-efficient of the EV.

The delay indicates the elapsed time after which the control signal arrives EV from EV aggregator. The delay can be expressed as an exponential mathematical function  $e^{-st(t)}$ , where  $\tau(t)$  indicate a time depedant funtion accounting signal delay time from EV aggregator to the EV. For simplified investigation, it is supposed that time constant  $T_{EV}$  and the delay time are same. For the EV aggregators the time varying delay is accounted by a sine wave function [20] with bias and amplitude taken as 1. For the scrutinized system the time varying delay is taken in the range [0,5s]. In the Fig.1,  $\alpha_1$  and  $\alpha_2$  are the participation factors for each generating unit of the dual-control area system. Two FNPID controllers are applied for smooth control of frequency in the designed unified model. The transfer function of all components of the system are shown in the Fig.1.

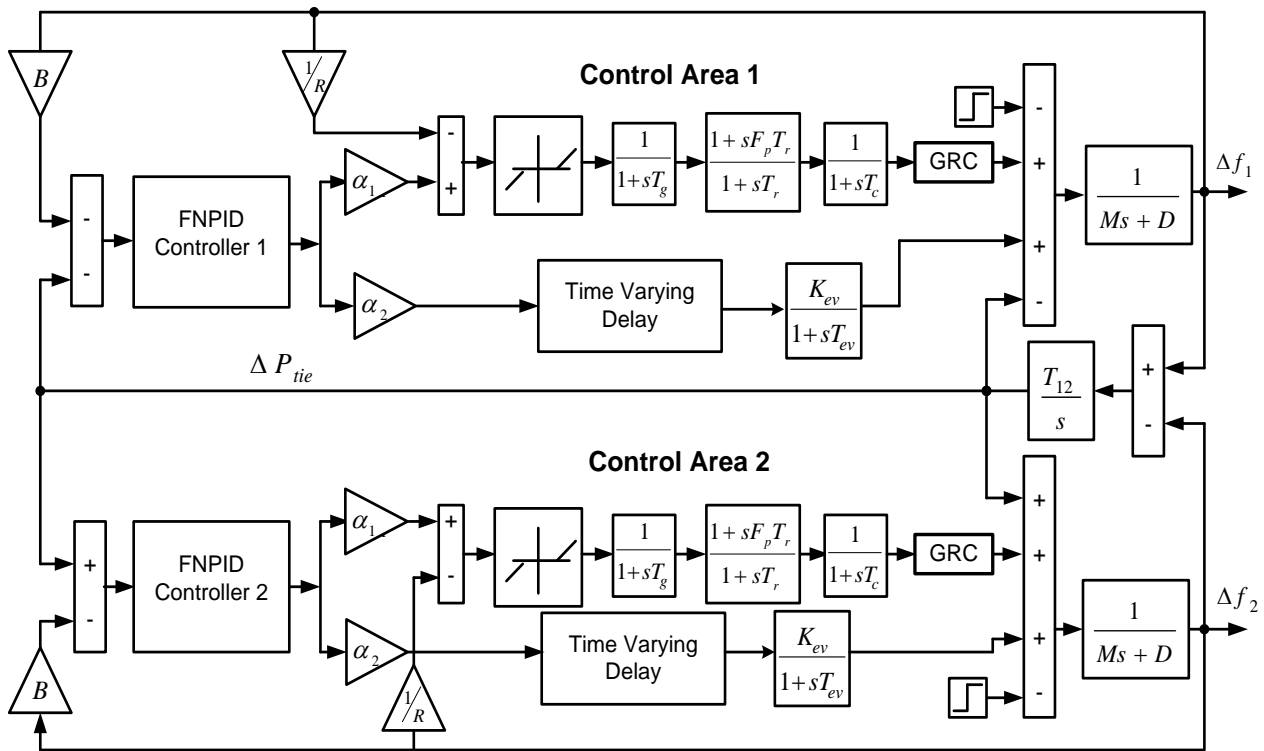


Figure 1. EV integrated power system represented by its transfer function

### 3. Methodology

#### 3.1 Multiverse Optimizer

Based on astrophysics an optimization technique is proposed by Mirjalili [27] known as Multi-Verse Optimizer. This method mainly based up on the interaction of countless universes in the form of white, black, and the wormholes, representing, respectively, the operations of exploring, exploiting, and searching locally. These three are the major

phases involved in the algorithm. The optimization process begins with the initialization of arbitrary variables called universes. During the progression of iteration, universe with improved fitness travel over black/white holes towards lower fitness valued universes. In the meantime each universe encounters a random theoretical changeover to the finest universe through wormholes. For mathematical formulation the roulette wheel is used as the tool for the movement of white/black holes in order to exchange the universe objects. In every iteration, universes get sorted based on the inflation

rates, and the roulette wheel's system detects a white hole and picks it up.

During the optimizing process, in the initial phase two variables need to be computed namely, Traveling Distance Rate (TDR) and Wormhole Existence Probability (WEP). This two variables decide the amount of updation of solutions during the optimization procedure. The mathematical definition of WEP and TDR are portrayed below.

$$WEP = a + t \times \frac{(b-a)}{T} \tag{1}$$

Here a, b and t respectively indicates the maximum, minimum and current iteration of the optimizing process. The maximum iteration count is denoted by T.

$$TDR = 1 - \frac{t^{1/p}}{T^{1/p}} \tag{2}$$

Exploitation accuracy is denoted by the symbol *p*. The Exploitation of the algorithm solely depends on its value.

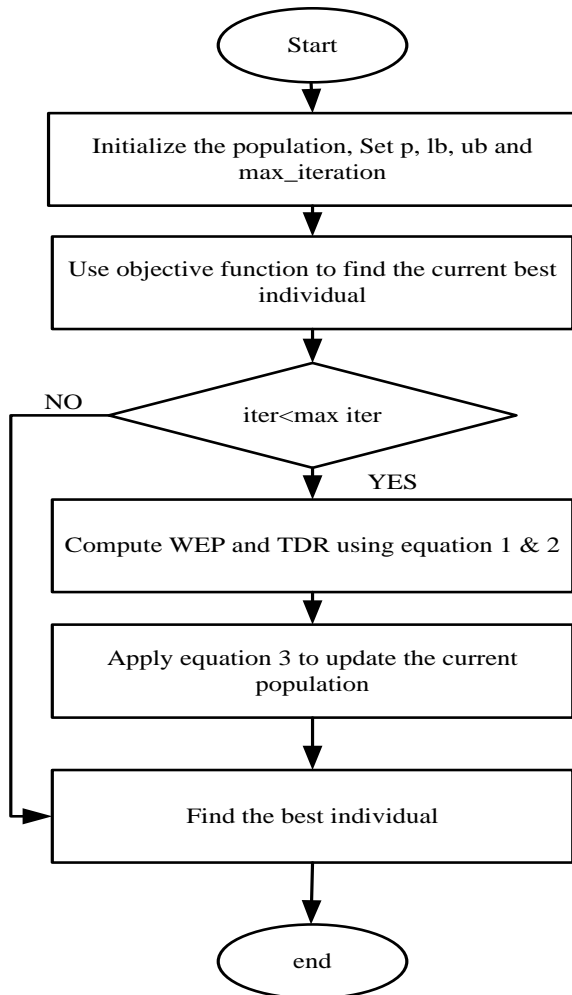


**Figure 2.** Flowchart explaining flow of MVO

After computing TDR and WEP, the initial population is updated using the below equation (3).

$$x_i^j = \begin{cases} x_i + TDR + ((ub_j - lb_j) * r_4 + lb_j) & \text{if } r_3 < 0.5 \text{ and } r_2 < WEP \\ x_i - TDR + ((ub_j - lb_j) * r_4 + lb_j) & \text{if } r_3 \geq 0.5 \text{ and } r_2 < WEP \\ x_{roulettewheel}^j & \text{if } r_2 \geq WEP \end{cases} \tag{3}$$

*j*th component of the best fitted solution is represented by  $x_j$ .  $lb_j$  and  $ub_j$  respectively denote the lower cap and upper cap of the *j*th element.  $r_2$ ,  $r_3$  and  $r_4$  denotes the random numbers in the segment [0,1].  $x_i^j$  denotes the *j*th component of *i*th solution. Roulette Wheel method is used to generate the *j*th component of the solution denoted by  $x_{roulettewheel}^j$ . The above equation (3) shows that solutions can be updated after calculating the previous best solution. The exploring, exploiting, and local searching of the optimizing process is confirmed by the equation (3). The Figure 2 depicts the flow of MVO process. The more details about MVO can be found in article [27].

**3.2 Controller Architecture**

**3.2.1 PID controller**

Input to a PID controller is the error between the desired and actual response and using appropriate control action it produces a suitable output to minimize the error in the output of the process. PID controller has three control actions namely: Proportional (P), Integral (I) and Derivative (D). ‘P’ produces a proportional control action to take care of the current error, ‘I’ produces an integral control action to take care of accumulated past errors and ‘D’ produces a derivative control action to take care of future errors that may occur in the system output. These three combined control actions make the process to produce the desired output. Figure 3 shows the internal arrangement of a PID controller.

Transfer function of the PID controller is given by,

$$C(s) = \frac{U(s)}{E(s)} = K_p + \frac{K_i}{s} + K_d s \tag{4}$$

Where  $K_p$ ,  $K_i$  and  $K_d$  are known as proportional gain, integral gain and derivative gain respectively.

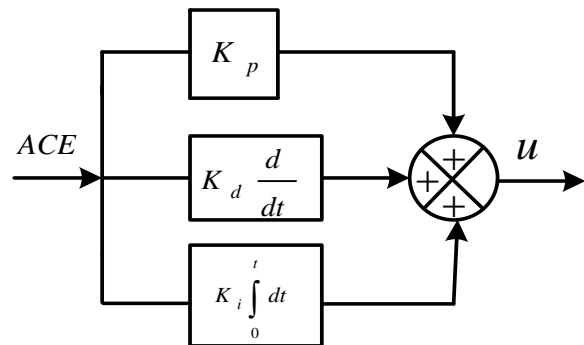


**Figure 3.** Internal Design of PID controller

**3.2.2 Fuzzy plus Non-Integer PID (FNPID) Controller**

The traditional Fuzzy-PID controller consists of four scaling factors ( $K_{f1}, K_{f2}, K_{f3}$  &  $K_{f4}$ ), integer order integral, derivative and proportional controller along with a fuzzy inference system. This means that the values of two tuning variables attached to the integral and derivative controller should have unity value i.e.  $\lambda = \mu = 1$ . In a Fractional calculus based Fuzzy-PID controller, the integral and derivative controllers come with two adjustable parameters  $\lambda$  and  $\mu$  and can have any values between 0 and 1. Keeping aside the stated differences, all other design aspects of a FNPID controller is exactly the identical as the traditional integer order Fuzzy-PID controller. Fuzzy-PID controller can be said to be a special case of FNPID when  $\lambda = \mu = 1$ . Figure 4 illustrates the structure of FNPID controller. The membership functions and rule-base of FNPID controller are depicted in Fig. 5 and Table.1 respectively. Here mamdani type fuzzy rules are considered for inference engine. There are five input and output membership functions (f1, f2, f3, f4, f5) which are of triangular shaped as depicted in Fig. 5. The inference engine considers 25 fuzzy IF-THEN rules which are tabulated in Table 1. Based on the proper adjustment of scaling factors and fuzzy rules the FNPID controller produces control output.

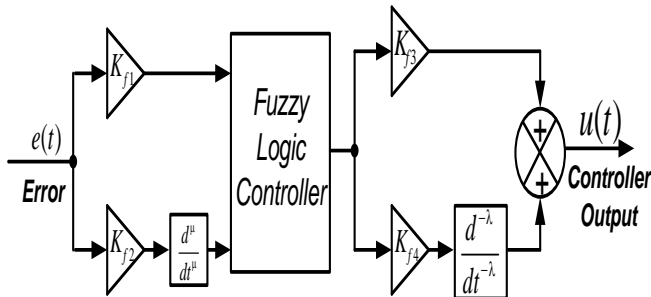


Figure 4. Internal Design of FNPID controller

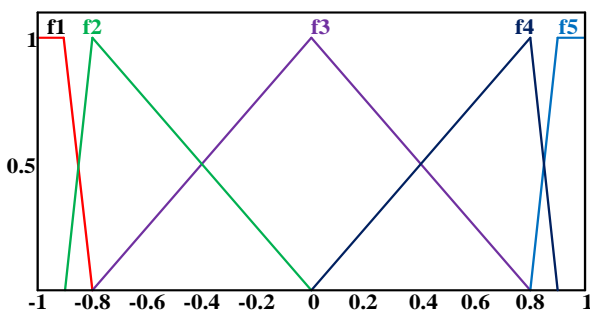


Figure 5. Membership function structure of FNPID controller

Table 1: Twenty-five rules of fuzzy structure of FNPID controller.

error	Δerror				
	f1	f2	f3	f4	f5
f1	f1	f1	f2	f2	f3
f2	f1	f2	f2	f3	f4
f3	f2	f2	f3	f4	f4
f4	f2	f3	f4	f4	f5

f5	f3	f4	f4	f5	f5
----	----	----	----	----	----

3.3 MVO applied to tune the proposed FNPID controller

The MVO technique is applied to adjust the gain factors of projected FNPID controllers. The following steps are followed to tune the controller parameters with MVO.

- i. A random population demonstrating controller parameters ( $K_{f1}, K_{f2}, K_{f3}, K_{f4}, \lambda, \mu$ ) is generated in the initial phase within the pre-decided range. The population dimension is set at  $100 \times 12$  associated with 12 gain factors of two FNPID controllers.
- ii. ITAE (equation 5) is considered as objective function to evaluate the randomly generated solutions.
- iii. Equations 1-2 are applied to compute WEP and TDR.
- iv. Equation 3 is applied to modify the existing population.
- v. Individual comparison is made between updated and previous version of population in terms of fitness function.
- vi. The individual having improved fitness will be allowed for next iteration.
- vii. Steps (ii) to (vi) are reiterated till 100 iterations (maximum iteration) are accomplished.
- viii. The optimum controller’s gain is chosen from the final population having best fitness value.

4. Result and Discussion

The multi-area EV incorporated model is examined by applying an unpredicted load fluctuation in control area 1. The constraints of the employed PID, FPID and FNPID controllers are adjusted by MVO technique with the application of 0.01 p.u. sharp load variation in control area 1. The ITAE also known as Integral Time Absolute Error (represented by equation 5) is act as fitness function for the said tuning process.

$$ITAE = \int_0^t (|\Delta f_1| + |\Delta f_2| + |\Delta P_{tie}|) dt \tag{5}$$

The examination can be carried out by applying a load deviation in any one of the control areas but here we have considered control area 1. The unified system is modelled with Simulink toolbox of MATLAB and the MVO is programmed in MATLAB. MVO is run for 20 times and best solutions are selected from that. The tuned controller constraints for all three types of controllers (FNPID, FPID & PID) obtained with MVO process are tabulated in Table 2. The capability of the controllers are judged by observing the oscillations of frequency in both control areas and interline power, portrayed by Fig.6, Fig.7 and Fig.8. These figures shows that the projected FNPID controller settles the oscillations of frequency in both control area and interline power faster than conventional FPID and PID controller. The mathematical computation of maximum positive deviation (overshoot), settling time and minimum negative deviation (undershoot) of system responses are carried out and tabulated in Table.3. The response of the system is said to be superior if it holds least values of undershoots, settling time and overshoots. Figures 6-8 and Table 3 witness the

supremacy of FNPID controller over FPID and PID controller as the projected FNPID controller possesses the least values of the response specifications as compared to other mentioned controllers.

Further the flexibility of the implemented FNPID controller is established by following robustness analysis.

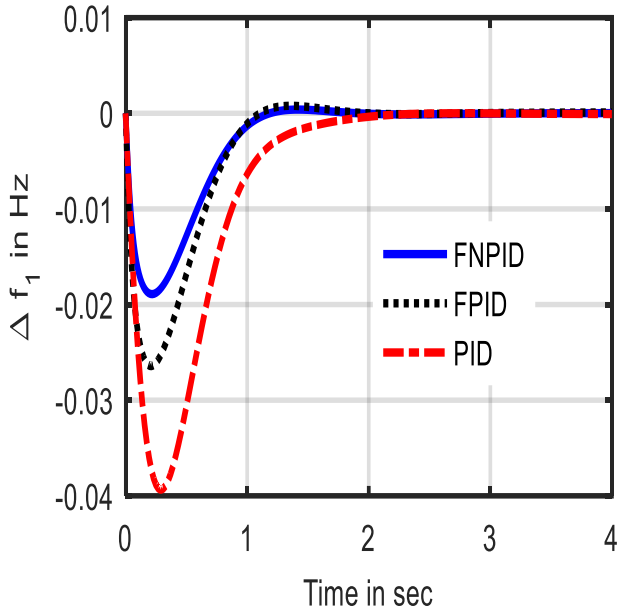


Figure 6. Oscillations of frequency of area 1 due to demand variation in control area 1

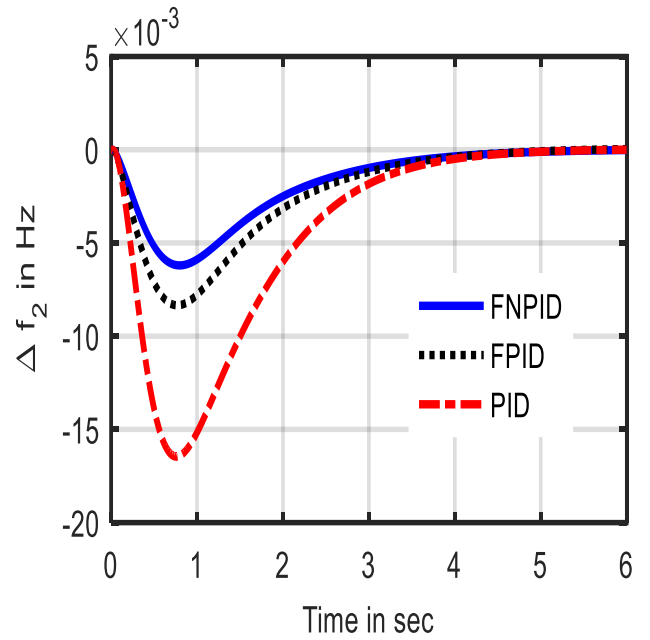


Figure 7. Oscillations of frequency of area 2 due to demand variation in control area 1

Table 2. MVO tuned optimum controller gains.

Controller	Control Area 1						Control Area 2					
	$K_{f1}$	$K_{f2}$	$K_{f3}$	$K_{f4}$	$\lambda$	$\mu$	$K_{f1}$	$K_{f2}$	$K_{f3}$	$K_{f4}$	$\lambda$	$\mu$
FNPID	1.584	0.997	1.874	1.142	0.87	0.98	1.956	0.578	1.147	1.886	0.79	0.85
FPID	1.025	1.114	1.596	1.854	NA	NA	1.875	1.012	1.547	1.257	NA	NA
PID	$K_p$		$K_i$		$K_d$		$K_p$		$K_i$		$K_d$	
	1.9765		0.4298		0.2899		1.4975		0.0110		0.5398	

Table 3. Response evaluative specifications of the scrutinised model with FNPID, FPID and PID controllers.

Controller	$\Delta P_{tie}$			$\Delta f_1$			$\Delta f_2$		
	$U_{sh}$	$T_s$	$O_{sh} \times 10^{-3}$	$U_{sh}$	$T_s$	$O_{sh} \times 10^{-3}$	$U_{sh}$	$T_s$	$O_{sh} \times 10^{-3}$
	in Hz	in sec	Hz	in Hz	in sec	Hz	in p.u.	in sec	p.u.
PID	-0.0077	3.0631	0.0979	-0.0394	1.8972	0.4242	-0.0165	3.9764	0.05752
FPID	-0.0054	3.0807	0.0172	-0.0264	1.5963	0.4034	-0.0083	3.7861	0.0341

<b>FNPID</b>	<b>-0.0040</b>	<b>3.0558</b>	<b>0.0105</b>	<b>-0.0189</b>	<b>1.0751</b>	<b>0.3888</b>	<b>-0.0062</b>	<b>3.6531</b>	<b>0.0300</b>
--------------	----------------	---------------	---------------	----------------	---------------	---------------	----------------	---------------	---------------

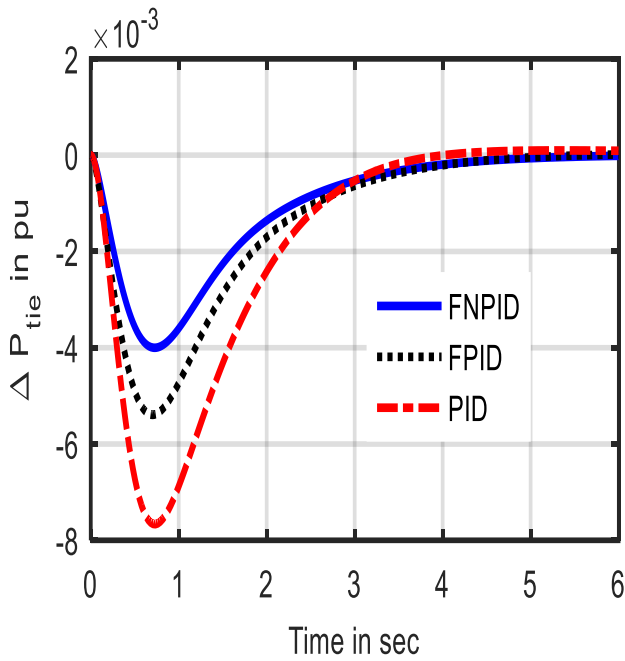


**Figure 8.** Oscillations of interline power due to demand variation in control area 1

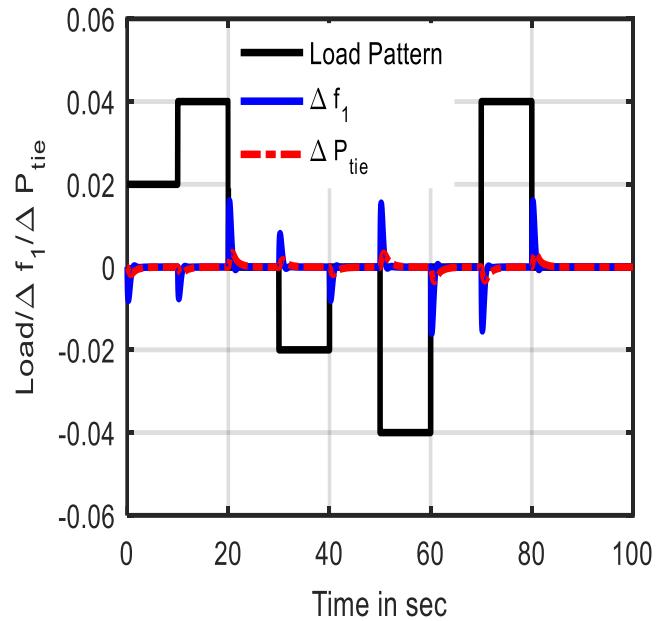


**Figure 9.** Oscillation of Interline power and area frequency due to random demand deviation.

4.1 Robustness analysis with Random demand variations:

The implemented FNPID controller in the multi-area system is considered to be robust if it can settle the abnormalities of any kind of unpredicted load fluctuations. To analyse this, the EV integrated model is subjected to random demand variations in control area 1 and the system responses are examined in terms of interline power oscillations and frequency deviations in both control areas. The shape of the random demand variations and system responses are displayed in Fig.9. This Figure evidences the robustness capability of the considered FNPID controller as it damps out the oscillations of frequency and interline power and make the system stable in a better manner.

4.2 Robustness analysis with System parameters variations:

As an extension of robustness check the constraints or the nominal parameters of the system are subjected to a wide range of deviations and the responses of the system are examined. Some constraints like R (regulation index) and B (bias index) of the examined model (Fig.1) are varied  $\pm 50\%$  and  $\pm 25\%$  and the performance evaluative indices i.e. maximum positive deviation(overshoot), settling time and minimum negative deviation(undershoot) are obtained and tabulated in Table 4. From these evaluative indices it can be seen that the maximum positive deviation (overshoot), settling time and minimum negative deviation (undershoot) are not changing widely even the constraints R and B are changing widely. The analysis again demonstrates the robustness behaviour of the projected FNPID controller

**Table 4.** Response evaluative specifications due to variation of system constraints.

System Constraints	%age variation	$U_{sh}$ for $\Delta f_1$ (in p.u.)	$T_s$ for $\Delta f_1$ (in sec)	$O_{sh} \times 10^{-3}$ for $\Delta f_1$ (in p.u.)	$U_{sh}$ for $\Delta P_{tie}$ (in p.u.)	$T_s$ for $\Delta P_{tie}$ (in sec)	$O_{sh} \times 10^{-3}$ for $\Delta P_{tie}$ (in p.u.)
<b>B</b>	-50%	-0.0199	1.0987	0.4015	-0.0061	3.1124	0.0415
	-25%	-0.0190	1.0897	0.3938	-0.0055	3.0987	0.0357
	+25%	-0.0175	1.0862	0.3745	-0.0051	3.0847	0.0225
	+50%	-0.0201	1.0945	0.4178	-0.0058	3.1021	0.0497
<b>R</b>	-50%	-0.0215	1.0975	0.4756	-0.0068	3.1985	0.0478
	-25%	-0.0201	1.0885	0.3978	-0.0059	3.0852	0.0364
	+25%	-0.0185	1.0897	0.3795	-0.0057	3.0975	0.0297

	+50%	-0.0200	1.0998	0.4221	-0.0062	3.1154	0.0496
--	------	---------	--------	--------	---------	--------	--------

## 5. Conclusion

The above research analysis confirmed the dominance of Fuzzy plus Non-Integer PID (FNPID) Controller over conventional FPID and PID controller in the multi generation unified power system. The multi-area model considered the nonlinear EV aggregators along with thermal power sources for evidencing the frequency deviation control. The result analysis and robustness analysis showed that the implemented FNPID controller successfully regulates the deviations of system frequency and interline power during unpredicted load disturbance in control areas. The random loading application and parameter alteration further proved the robustness of the projected FNPID Controller. Response specifications like maximum positive deviation (overshoot), settling time and minimum negative deviation (undershoot) are calculated for evidencing the dominance of the said FNPID controller over FPID and PID controllers.

## Appendix

Nominal Values of the constraints of the scrutinized model:  
 $M = 8.8$ ;  $T_g = 0.2$ ;  $T_r = 12$ ;  $T_c = 0.3$ ;  $D = 1$ ;  $F_p = 1/6$ ;  $T_{ev} = 0.1$ ;  $K_{ev} = 1$ ;  $B = 21$ ;  $R = 1/11$ ;  $\alpha_2 = 0.4$ ;  $\alpha_1 = 0.6$ ;  $T_{12} = 2$ .

## References

- [1] O.I. Elgerd, *Electric Energy Systems Theory. An introduction*. New Delhi: Tata McGraw-Hill; 1983.
- [2] N. Jaleeli, Louis S. VanSlyck, Donald N. Ewart, Lester H. Fink, and Arthur G. Hoffmann, "Understanding automatic generation control", *IEEE transactions on power systems*, Vol.7, No. 3, pp.1106-1122, 1992.
- [3] J. Nanda, A. Mangla, and S. Suri, "Some new findings on automatic generation control of an interconnected hydrothermal system with conventional controllers", *IEEE Transactions on energy conversion*, Vol. 21, No. 1, pp.187-194, 2006.
- [4] L. C. Saikia, J. Nanda, and S. Mishra, "Performance comparison of several classical controllers in AGC for multi-area interconnected thermal system", *International Journal of Electrical Power & Energy Systems*, Vol.33, No. 3, pp.394-401, 2011.
- [5] Mudi KR, Pal RN. A robust self-tuning scheme for PI-and PD-type fuzzy controllers. *IEEE Transactions on fuzzy system* 1999; 7:2–16.
- [6] R. J. Abraham, D. Das, and A. Patra, "Automatic generation control of an interconnected hydrothermal power system considering superconducting magnetic energy storage", *International Journal of Electrical Power & Energy Systems*, Vol.29, No. 8, pp.571-579, 2007.
- [7] R. J. Abraham, D. Das, and A. Patra, "Effect of TCPS on oscillations in tie-power and area frequencies in an interconnected hydrothermal power system", *IET Generation, Transmission & Distribution*, Vol.1, No. 4, pp.632-639, 2007.
- [8] H. Golpira, and H. Bevrani, "Application of GA optimization for automatic generation control design in an interconnected power system", *Energy Conversion and Management*, Vol.52, No. 5, pp.2247-2255, 2011.
- [9] S. P. Ghoshal, "Optimizations of PID gains by particle swarm optimizations in fuzzy based automatic generation control", *Electric Power Systems Research*, Vol.72, No. 3, pp.203-212, 2004.
- [10] M. Farahani, S. Ganjefar, and M. Alizadeh, "PID controller adjustment using chaotic optimisation algorithm for multi-area load frequency control", *IET Control Theory & Applications*, Vol.6, No. 13, pp.1984-1992, 2012.
- [11] E. Çam, and I. Kocaarslan, "Load frequency control in two area power systems using fuzzy logic controller", *Energy conversion and Management*, Vol.46, No. 2, pp.233-243, 2005.
- [12] S. R. Khuntia, and S. Panda, "Simulation study for automatic generation control of a multi-area power system by ANFIS approach", *Applied soft computing*, Vol.12, No. 1, pp.333-341, 2012.
- [13] Z. Ziadi, A. Yona, T. Senjyu, M. Abdel-Akher, & T. Funabashi, "Real time voltage control of unbalanced distribution systems with photovoltaic generation", *Renewable Energy Research and Applications (ICRERA)*, International Conference on. IEEE, pp. 1-6, November 2012.
- [14] M. K. Debnath, R. K. Mallick, and B. K. Sahu, "Application of hybrid differential evolution–grey wolf optimization algorithm for automatic generation control of a multi-source interconnected power system using optimal fuzzy–PID controller", *Electric Power Components and Systems*, Vol.45, No. 19, pp.2104-2117, 2017.
- [15] I. Pan, and S. Das, "Fractional order AGC for distributed energy resources using robust optimization", *IEEE transactions on smart grid*, Vol.7, No. 5, pp.2175-2186, 2015.
- [16] M.K. Debnath, S. Sinha, and R. K. Mallick, "Automatic Generation Control Including Solar Thermal Power Generation with Fuzzy-PID controller with Derivative Filter", *International Journal of Renewable Energy Research (IJRER)*, Vol.8, No. 1, pp: 26-35, 2018.
- [17] J. Morsali, K. Zare, and M. T. Hagh, "A novel dynamic model and control approach for SSSC to contribute effectively in AGC of a deregulated power system", *International Journal of Electrical Power & Energy Systems*, Vol.95, pp.239-253, 2018.
- [18] N. C. Patel, M. K. Debnath, B. K. Sahu, S. S. Dash, & R. Bayindir, "Multi-Stage PID Controller Tuned by Invasive Weed optimization Algorithm for LFC Issues", 2018 7th International Conference on Renewable Energy Research and Applications (ICRERA), IEEE, pp. 1358-13, 2018.



- [19] P. C. Sahu, S. Mishra, R. C. Prusty, and S. Panda, "Improved-salp swarm optimized type-II fuzzy controller in load frequency control of multi area islanded AC microgrid", *Sustainable Energy, Grids and Networks*, Vol.16, pp.380-392, 2018.
- [20] N. C. Patel, B. K. Sahu, and M. K. Debnath, "Automatic generation control analysis of power system with nonlinearities and electric vehicle aggregators with time-varying delay implementing a novel control strategy", *Turkish Journal of Electrical Engineering and Computer Sciences*, Vol.27, No. 4, pp.3040-3054, 2019.
- [21] G. Mohapatra, M. K. Debnath, and K. K. Mohapatra, "IMO-based novel adaptive dual-mode controller design for AGC investigation in different types of systems", *Cogent Engineering*, Vol.7, No. 1, pp.1711675, 2020.
- [22] A. Bagheri, A. Jabbari, and S. Mobayen, "An intelligent ABC-based terminal sliding mode controller for load-frequency control of islanded micro-grids", *Sustainable Cities and Society*, Vol.64, pp.102544, 2021.
- [23] S. Bhongade, and V. P. Paramar. "Automatic generation control of two-area ST-Thermal power system using jaya algorithm", *International Journal of Smart Grid*, Vol.2, No. 2, pp.99-110, 2018.
- [24] E. Çelik, "Design of new fractional order PI–fractional order PD cascade controller through dragonfly search algorithm for advanced load frequency control of power systems", *Soft Computing*, Vol.25, No.2, pp.1193-1217, 2021.
- [25] D. Guha, P. K. Roy, and S. Banerjee, "Equilibrium optimizer-tuned cascade fractional-order 3DOF-PID controller in load frequency control of power system having renewable energy resource integrated", *International Transactions on Electrical Energy Systems*, Vol.31, No.1, pp.e12702, 2021.
- [26] N. K. Jena, S. Sahoo, B. K. Sahu, and K. B. Mohanty, "Design of fractional order cascaded controller for AGC of a deregulated power system", *Journal of Control, Automation and Electrical Systems*, Vol.33, No. 5, pp.1389-1417, 2022.
- [27] S. Mirjalili, S. M. Mirjalili, and A. Hatamlou, "Multi-verse optimizer: a nature-inspired algorithm for global optimization", *Neural Computing and Applications*, Vol.27, No. 2, pp.495-513, 2016.
- [28] M. W. Siti, D. H. Tungadio, N. T. Nsilulu, B. B. Banza, and L. Ngoma, "Application of load frequency control method to a multi-microgrid with energy storage system", *Journal of Energy Storage*, Vol.52, pp.104629, 2022.
- [29] M. Ahmed, G. Magdy, M. Khamies, and S. Kamel, "Modified TID controller for load frequency control of a two-area interconnected diverse-unit power system", *International Journal of Electrical Power & Energy Systems*, Vol.135, pp.107528, 2022.
- [30] M. O. A. Kader, K. T. Akindeji, and G. Sharma, "Application of PHEVs Influence on Frequency Regulation of a Two Area Power System", In *2022 10th International Conference on Smart Grid (icSmartGrid)*, IEEE, pp. 23-28, 2022.